

1-1-2001

H α Imaging with Hubble Space Telescope-Nicmos of an Elusive Damped Iy α Cloud at $z = 0.6^1$

Nicolas Bouché

University of Massachusetts Amherst

James D. Lowenthal

University of Massachusetts Amherst, jlowenth@smith.edu

Jane C. Charlton

Pennsylvania State University

Matthew A. Bershad

University of Wisconsin-Madison

Christopher W. Churchill

*Pennsylvania State University**See next page for additional authors*Follow this and additional works at: https://scholarworks.smith.edu/ast_facpubsPart of the [Astrophysics and Astronomy Commons](#)

Recommended Citation

Bouché, Nicolas; Lowenthal, James D.; Charlton, Jane C.; Bershad, Matthew A.; Churchill, Christopher W.; and Steidel, Charles C., "H α Imaging with Hubble Space Telescope-Nicmos of an Elusive Damped Iy α Cloud at $z = 0.6^1$ " (2001). Astronomy: Faculty Publications, Smith College, Northampton, MA. https://scholarworks.smith.edu/ast_facpubs/63

This Article has been accepted for inclusion in Astronomy: Faculty Publications by an authorized administrator of Smith ScholarWorks. For more information, please contact scholarworks@smith.edu

Authors

Nicolas Bouché, James D. Lowenthal, Jane C. Charlton, Matthew A. Bershady, Christopher W. Churchill, and Charles C. Steidel

EXTRAORDINARY LINE-EMITTING KNOTS IN THE CRAB NEBULA¹

GORDON M. MACALPINE, STEPHEN S. LAWRENCE, AND BETH A. BROWN
 Department of Astronomy, University of Michigan, Ann Arbor, MI 48109

ALAN UOMOTO
 Department of Physics and Astronomy, The Johns Hopkins University, Baltimore, MD 21218

BRUCE E. WOODGATE, LARRY W. BROWN, AND RONALD J. OLIVERSEN
 Goddard Space Flight Center, Greenbelt, MD 20771

JAMES D. LOWENTHAL
 Lick Observatory, University of California, Santa Cruz, CA 95064

AND

CHARLES LIU
 Department of Astronomy, University of Arizona, Tucson, AZ 85721
 Received 1994 February 28; accepted 1994 June 21

ABSTRACT

Extraordinary, semistellar, line-emitting knots are apparent in images of the Crab Nebula which were obtained with the Goddard Fabry-Perot imager at the Michigan-Dartmouth-MIT Observatory. The knots are most prominent for [O III] $\lambda 5007$ emission through a 5.3 \AA (FWHM) bandpass centered at 5015.3 \AA , with representative fluxes of roughly $10^{-14} \text{ ergs cm}^{-2} \text{ s}^{-1}$. They are aligned in arcs, seven to the north and four to the south, from the pulsar. The northern group appears to be in a bounded corridor through the filamentary structure. Measurements over a 2 year baseline yield proper motions of order $0''.1 \text{ yr}^{-1}$, corresponding to transverse velocities of order 900 km s^{-1} for a distance of 1830 pc. The knots are characterized by remarkably strong [Ar III] emission, possibly indicating high argon abundances, high gas temperatures, or anomalous physical processes.

Subject headings: ISM: individual (Crab Nebula) — pulsars: individual (PSR 0531 + 21) — supernova remnants

1. INTRODUCTION

Relatively recent studies have demonstrated that the Crab Nebula filaments have large-scale, north-south bipolar structure, constricted in the east-west plane by a torus of line-emitting gas (Uomoto & MacAlpine 1987, hereafter UM; MacAlpine et al. 1989, hereafter MMMU; Michel et al. 1991; Fesen, Martin, & Shull 1992). Figure 3 of UM provides a striking, two-dimensional illustration of the structure. It shows the north-south lobes and the east-west “band” with exceptionally high helium abundance, whose toroidal nature (around the pulsar) was first postulated by MMMU. Further evidence for the nebula’s bipolar form is provided by the hourglass pattern seen in polarized light by Michel et al., who also spoke of a toroidal emission region surrounding the pulsar; and a similar geometry was discussed by Fesen et al., who postulated a magnetic torus around the emission tori of MMMU and Michel et al. It would be worthwhile to search for other north-south axial phenomena, possibly directly associated with the Crab Nebula pulsar. This paper reports the detection of extraordinary knots of line-emitting gas in remarkable alignment to the north and south from the pulsar vicinity.

2. OBSERVATIONS

As part of a project aimed at developing three-dimensional, line-emission data cubes for the Crab Nebula, images were

obtained at the Michigan-Dartmouth-MIT Observatory using the Goddard Fabry-Perot imager (GFPI). The GFPI, which incorporates Queensgate etalons and a Tektronix 512×512 CCD, is well described by Caulet et al. (1992). The series of line-emitting knots was first noticed in an [O III] $\lambda 5007$ image obtained in 1989 December at the McGraw-Hill 1.3 m telescope. The bandpass of the etalon was set to 320 km s^{-1} FWHM and centered at 5015.3 \AA . The knots were also visible, though not as conspicuous as a group, on frames centered at 5011.2 , 5013.2 , and 5017.6 \AA . Integration times were 300 s, the image scale was $0''.84 \text{ pixel}^{-1}$, and the seeing was measured at $2''.7$. Additional 320 km s^{-1} bandpass images near 5015.3 \AA were acquired in 1991 November and 1993 December with the GFPI mounted on the Hiltner 2.4 m telescope. With a scale of $0''.46 \text{ pixel}^{-1}$, the field of view was only $3'55''$ on a side, centered on the north-central portion of the nebula. These 600 s exposures were taken when the seeing was about $2''.0$.

Initial data reductions followed standard procedures for CCD images, employing routines in the IRAF software package.² Each image was edited for defects and cosmic rays, bias-subtracted, and flattened. Individual 1989 frames were normalized to a common level by assuming stars within the field of view have relatively uniform spectra in the narrow range of wavelengths considered. The absolute flux calibration was obtained from standard star (Massey et al. 1988) images taken through the same etalon spacings as object frames.

¹ Based in part on research carried out at the MDM Observatory, operated by the University of Michigan, Dartmouth College, and the Massachusetts Institute of Technology.

² The Image Reduction and Analysis Facility (IRAF) is distributed by the Association of Universities for Research in Astronomy, Inc., under contract to the National Science Foundation.

Finally, the synchrotron continuum emission was removed from the 1989 images by subtracting frames sufficiently displaced in wavelength from emission lines.

Spectroscopy of some of the knots was acquired in 1993 March at the Hiltner 2.4 m telescope, using the Mark III spectrograph with a Loral 2048 × 2048 CCD. A slit width of 1".68, a 300 line mm⁻¹ grism blazed at 8000 Å and an RG610 filter yielded 6100–10000 Å coverage with 3 Å pixel⁻¹ dispersion. Also, a slit width of 1".17 was used with a 600 line mm⁻¹ grism blazed at 4600 Å to obtain 4200–7200 Å coverage at 1.5 Å pixel⁻¹. Total exposure times were 45–60 minutes, during which sky conditions were nonphotometric. All spectroscopic data were fully reduced using IRAF software.

3. DISCUSSION

The 1991 Fabry-Perot image obtained at the 2.4 m telescope and showing the north-central region of the Crab Nebula is presented in Figure 1 (Plate L13). This frame has only been bias-subtracted and flattened. In the corresponding diagram of Figure 2, positions of stars are represented by filled circles with numbers as assigned by Wyckoff & Murray (1977, hereafter WM), and the pulsar is labeled P. The knots are represented by plus signs and are labeled sequentially to the north and south from the pulsar. It may be seen that most of the knots have semistellar appearances, and they are conspicuously aligned,

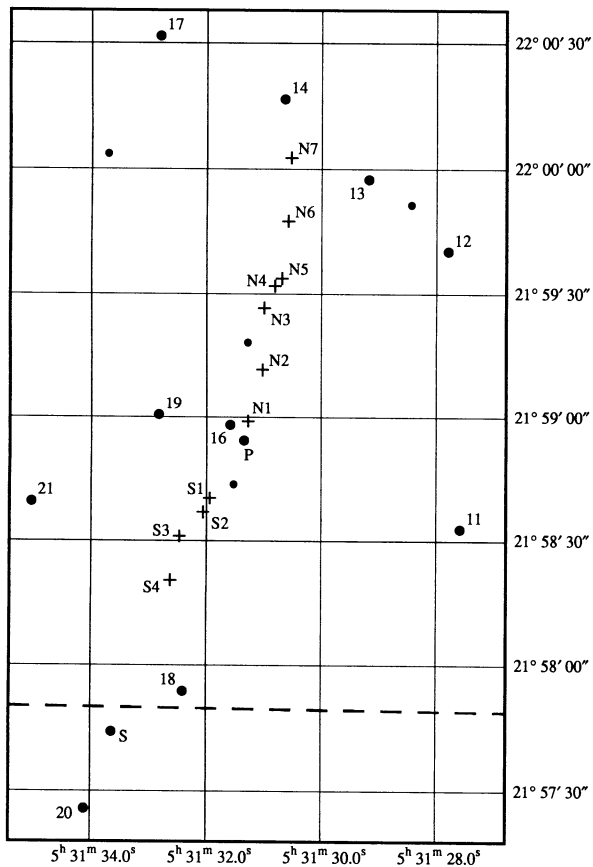


FIG. 2.—Positional diagram for stars and knots in Fig. 1 (Plate L13). The axes are labeled with right ascension (*abscissa*) and declination (*ordinate*). Stars are represented with filled circles, most of which are labeled with numbers as assigned by WM, and knots are represented with plus signs. The boundaries of this diagram do not coincide with the boundaries of Fig. 1, the southern edge of which falls along the dashed line.

seven to the north and four to the south. The overall alignment is roughly perpendicular to the high-helium torus detected by UM. The northern sequence appears to be situated in a corridor through filamentary structure. To provide some points of reference, we note that the west-directed appendage located east of WM star 14 (see Figs. 1 and 2) coincides with the northern nickel- and iron-rich arch discussed by MMMU; and the eastern side of the apparent corridor at the top of Figure 1 merges into the western edge of the well-known “jet” discovered by van den Bergh (1970). This corridor containing the knots is suggestive of a north-south-directed, collimated wind coming from the pulsar vicinity.

Criteria for identifying and labeling knots, as described above, included semistellar and/or isolated appearance, as well as alignment to the north or south from the pulsar. Other fainter and less distinctive gas condensations may also be present in Figure 1 to the south and 11" west of the pulsar.

In the sequence of 1989 1.3 m telescope images wherein the knots were originally detected, the knots are confined to a small range in velocity along the line of sight. Each appears, becomes most prominent, and then disappears within four of the 320 km s⁻¹ velocity slices, spaced approximately 120 km s⁻¹ apart. By comparing the measured intensity of each knot from frame to frame, dominant radial velocities were derived for all cases (with estimated uncertainties of 80 km s⁻¹), and somewhat more accurate values (to within 40 km s⁻¹) have been measured spectroscopically for knots N2, N3, N5, and N6. The velocities are given in column (2) of Table 1, and they range from +300 to +720 km s⁻¹, with no obvious correlation between radial velocity and distance from the pulsar. As mentioned previously, the aligned knots north of the pulsar are most easily seen in the frame centered at 5015.3 Å (+505 km s⁻¹). Their visibility drops dramatically in a 5019.6 Å (+760 km s⁻¹) image, and then a spatially coincident filament shines brightly in a 5026.0 Å (+1145 km s⁻¹) frame. The apparent spatial association of aligned knots and the filament may not be significant, given the large radial velocity difference. However, it is plausible that the knots have resulted from instabilities (e.g., Rayleigh-Taylor or Kelvin-Helmholtz) involving the filament. We note that we did not find evidence for aligned, isolated knots at any other positions or velocity cuts. Perhaps this filament is unique in being situated at the

TABLE 1
KNOT RADIAL VELOCITIES, POSITIONS, AND PROPER MOTIONS

Knot (1)	V_{rad} (km s ⁻¹) (2)	X^a (3)	Y^b (4)	ΔX^c (5)	ΔY^c (6)	μ (yr ⁻¹) (7)
N1	660	-4.3	0.9	0.1	0.1	0.07
N2	500	-7.8	13.5	0.0	0.1	0.05
N3	720	-8.2	28.5	-0.1	0.0	0.05
N4	...	-10.8	33.8	(-0.1)	(0.2)	(0.11)
N5	530	-12.5	35.6	-0.1	0.1	0.07
N6	300	-14.0	49.4	0.0	0.2	0.10
N7	510	-14.7	64.6	(0.0)	(0.2)	(0.10)
S1	420	5.0	-17.8	0.0	0.0	0.00
S2	720	6.5	-21.2	0.1	-0.1	0.07
S3	630	12.2	-27.0	0.0	-0.2	0.10
S4	400	14.5	-37.6	0.0	-0.2	0.10

^a Position offset (positive X eastward) relative to WM star 16 at $\alpha_{1950.0} = 5^{\text{h}}31^{\text{m}}31^{\text{s}}.56$.

^b Position offset (positive Y northward) relative to WM star 16 at $\delta_{1950.0} = +21^{\circ}58'58''.0$.

^c Measured in the sense of (position in 1993.92) - (position in 1991.87).

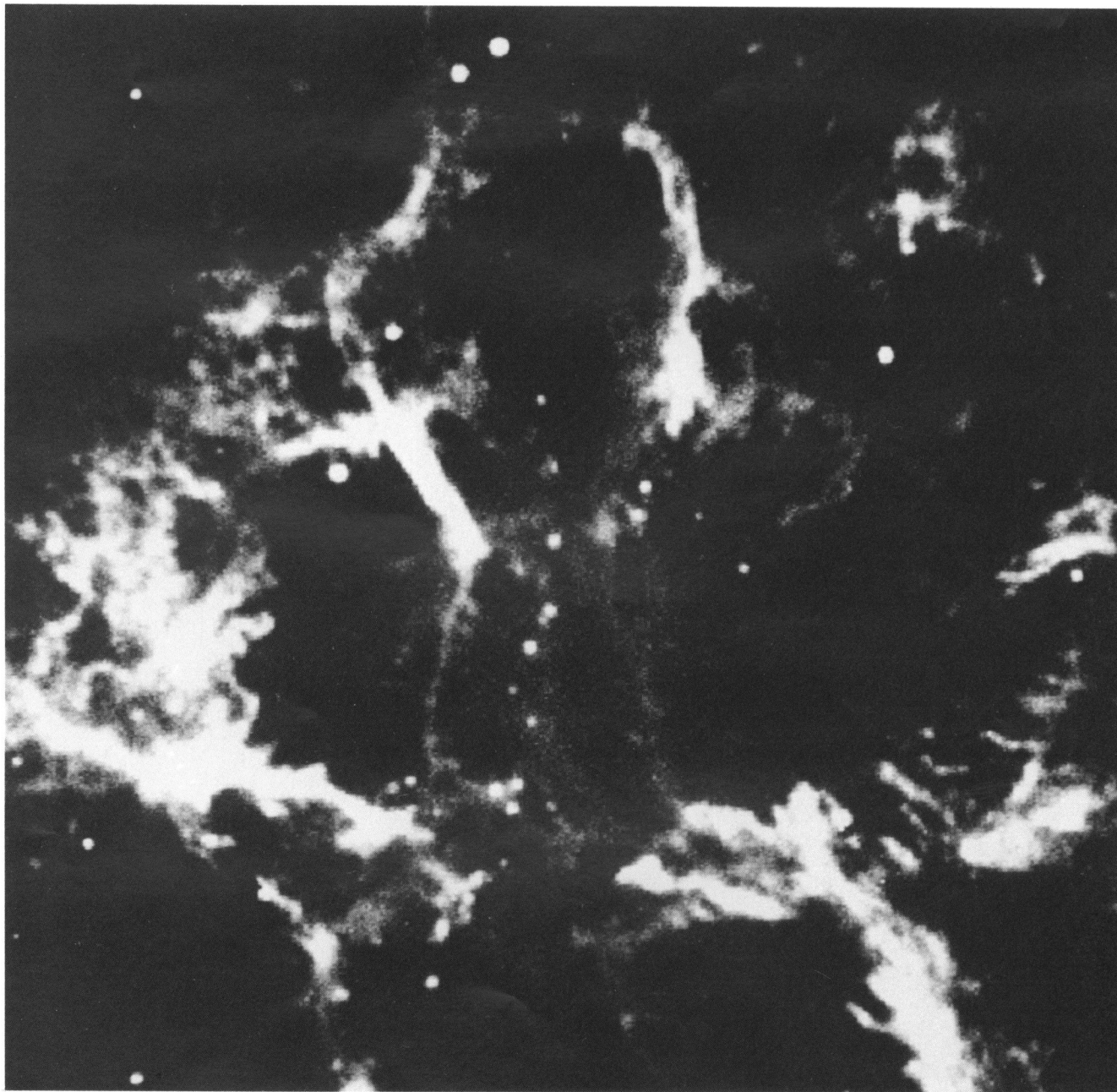


FIG. 1.—[O III] $\lambda 5007$ image of the north-central part of the Crab Nebula, obtained in 1991 with the GFPI on the Hiltner 2.4 m telescope. The bandpass is 5.3 \AA centered at 5015.3 \AA . North is up, east is to the left, and the field is $3'55''$ on a side.

MACALPINE et al. (see 432, L132)

edge of a collimated wind, resulting in Kelvin-Helmholtz instabilities; or the knots may be a consequence of our line of sight being aligned with the long axes of Rayleigh-Taylor appendages protruding from the filament.

Measured fluxes of the knots in [O III] $\lambda 5007$, through the 320 km s^{-1} bandpass in the calibrated 1989 data, range from 3×10^{-15} to $5 \times 10^{-14} \text{ ergs cm}^{-2} \text{ s}^{-1}$. The knots are also present in [S II] $\lambda\lambda 6716, 6731$ images for the same velocity bandpass and with estimated observed flux levels of order $10^{-14} \text{ ergs cm}^{-2} \text{ s}^{-1}$. However, they are not seen in GFPI images of H β , He I $\lambda 5876$, or [Ni II] $\lambda 7378$, suggesting upper limits of roughly several times $10^{-16} \text{ ergs cm}^{-2} \text{ s}^{-1}$ for these lines.

Using stellar coordinate data from WM and an IRAF centroiding algorithm, accurate knot positions were measured for the +505 km s^{-1} frames taken in 1991 and 1993 (which have more suitable resolution than the 1989 frame). The measurements over a 2 year baseline yielded position changes up to $0''.2$, with uncertainties of $0''.1$. Columns (3) and (4) of Table 1 contain knot position offsets relative to star 16 of WM (measured from the 1991 image), while columns (5) and (6) show the 2 year position changes. In column (7), we give the resultant proper motions, which have $0''.07 \text{ yr}^{-1}$ uncertainties. All derived proper motions are less than or of order $0''.1 \text{ yr}^{-1}$, suggesting tangential velocities less than or of order 900 km s^{-1} for a distance to the Crab Nebula of 1830 pc (Davidson & Fesen 1985). Data in parentheses have larger than average uncertainty due to knot faintness or poor definition. All measured north or south motions are directed away from the pulsar, as expected.

Spectra of the knots have remarkably strong [Ar III] and [S II] emission. The strengths of these lines for the best observed knot (N6) are illustrated in Figure 3, which shows the 6400–7200 Å spectral range. The H α and [N II] emission-line complex contains significant contributions from knot N6, the nebular nearside (roughly -1260 km s^{-1}), and the nebular backside (roughly $+1220 \text{ km s}^{-1}$). On the other hand, [S II] and especially [Ar III] emission are dominated solely by the knot (an “argoknot”). Selected, measured knot N6 line fluxes for the entire observed spectral range, relative to H β , are presented in Table 2. Estimated measurement uncertainties are

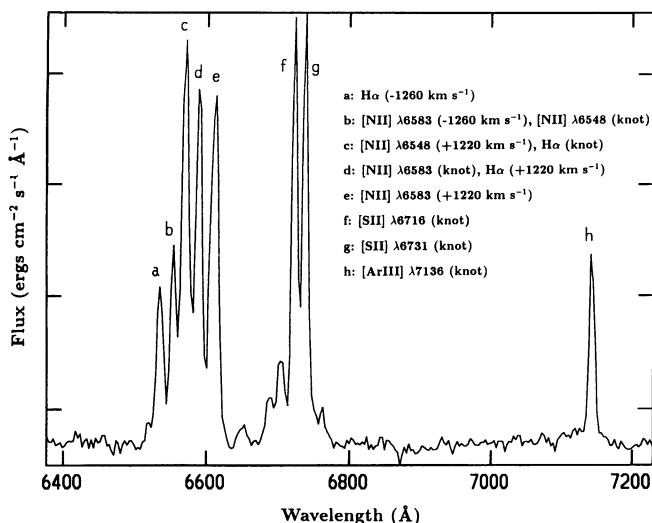


FIG. 3.—Spectrum of knot N6 in the range 6400–7200 Å. Stronger emission lines are labeled.

TABLE 2
RELATIVE LINE INTENSITIES

LINE	KNOT N6		SOUTHERN POSITION	
	F ^a	I ^b	F ^a	I ^b
H γ	0.50	0.61
[O III] 4363	0.27	0.34
He II 4686	0.94	1.0	0.43	0.46
H β	1.0	1.0	1.0	1.0
[O III] 5007	15	14	6.9	6.5
[O I] 6300	0.87	0.55	2.4	1.5
[N II] 6548	3.0	1.8	0.96	0.58
H α	7.6	4.5	6.9	4.1
[S II] 6716	8.7	5.0	14	8.3
[Ar III] 7136	4.1	2.2	1.9	1.1

^a Flux measured relative to H β = 1.0.

^b Intensity corrected for $E_{B-V} = 0.47$, relative to H β = 1.0.

15% or less. We were able to derive $F(\text{H}\alpha)$ and $F([\text{N II}] \lambda 6548)$ by carefully deblending lines and using the known theoretical ratio of [N II] $\lambda 6548/\lambda 6583$. Due to faintness of the knots and declining spectrograph response toward shorter wavelengths, we were not able to measure lines shortward of 4500 Å. Also presented in Table 2 are relative line intensities after correction for a color excess of 0.47 (Davidson & Fesen 1985). We note that the identification of [Ar III] $\lambda 7136$ is secure because [Ar III] $\lambda 7751$ is also observed, with the theoretically expected $\lambda 7136/\lambda 7751$ ratio of approximately 4.

The exceptional strength of the [Ar III] emission is more remarkable than that of [S II], because the latter is known to be enhanced in filaments with broad low-ionization regions (see Henry & MacAlpine 1982). The intensity of [Ar III] emission, produced by collisions with thermal electrons, should scale with a recombination Balmer line in accordance with

$$\frac{I([\text{Ar III}] \lambda 7136)}{I(\text{H}\beta)} = \frac{N(\text{Ar}^{+2}) \nu_{7136}}{N(\text{H}^+) \nu_{4861}} \times \frac{8.63 \times 10^{-6} T^{-0.5} (\Omega/\omega) e^{-\Delta E/kT}}{\alpha_{\text{H}\beta}}, \quad (1)$$

where $N(\text{Ar}^{+2})$ and $N(\text{H}^+)$ are number densities, ν is photon frequency, T is electron temperature, Ω and ω are the argon line collision strength and lower level statistical weight, respectively, $\alpha_{\text{H}\beta}$ is the H β line effective recombination coefficient, and the exponential is the Boltzmann factor for collisional excitation of the argon line. Assuming collisional de-excitation to be negligible (which is valid for $N \ll 10^7 \text{ cm}^{-3}$) and letting $\alpha_{\text{H}\beta} = 1.61 \times 10^{-14} (2 \times 10^4/T)^{0.9} \text{ cm}^3 \text{ s}^{-1}$, we can simplify expression (1) to show its explicit temperature and ionization (or abundance) dependence:

$$\frac{I([\text{Ar III}] \lambda 7136)}{I(\text{H}\beta)} = \frac{N(\text{Ar}^{+2})}{N(\text{H}^+)} 2.58 \times 10^4 T^{0.4} e^{-20160/T}. \quad (2)$$

The strength of [Ar III] emission from knot N6 indicates that either the $N(\text{Ar}^{+2})/N(\text{H}^+)$ ratio there is a factor of 5–10 times higher than in more typical Crab Nebula filaments, N6 is characterized by surprisingly high gas temperature as suggested by MacAlpine, Lawrence, & Brown (1993), or the [Ar III] emission arises primarily from processes which are not normally important in nebular astrophysics. To investigate the temperature hypothesis, we remeasured [Ar III] $\lambda 7136/\text{H}\beta$ and also

the temperature-sensitive [O III] $\lambda 4363/\lambda 5007$ ratio in a relatively bright, Crab Nebula southern position previously reported to show unusually strong [Ar III] $\lambda 7136$ by MMMU (see their Fig. 7*b*). This location, toward which the southern knots appear to be directed, is just to the south of a star with coordinates $\alpha_{1950} = 05^{\text{h}}31^{\text{m}}33^{\text{s}}.62$ and $\delta_{1950} = +21^{\circ}57'44''.1$ (labeled "S" on Fig. 2). Its relative line intensities are also presented in Table 2, from which an [O III] gas temperature of 28,000 K may be deduced (see Osterbrock 1989). Then $N(\text{Ar}^{+2})/N(\text{H}^{+}) = 1.46 \times 10^{-6}$ may be derived using equation (2) above. Assuming a similar $N(\text{Ar}^{+2})/N(\text{H}^{+})$ value for knot N6 implies T of order 60,000 K there. This is significantly hotter than what would be expected from photoionization heating alone, further suggesting that the knots may be influenced by an energetic wind. Potential heating processes include shocking, Coulomb interactions, and collective effects as discussed by Scott et al. (1980). The [S II] $\lambda 6716/\lambda 6731$ ratio for N6 is measured to be 1.1, implying an electron density near 400 cm^{-3} for $T = 10,000 \text{ K}$, or 1000 cm^{-3} for $T = 60,000 \text{ K}$ (see Osterbrock 1989). The above temperature derivation is

very uncertain, because processes like collisional ionization and dielectronic recombination are assumed to have opposing effects so that $N(\text{Ar}^{+2})/N(\text{H}^{+})$ remains roughly constant over the 28,000–60,000 K range. We also assumed the knot hydrogen gas to be totally ionized, so Balmer line collisional excitation could be neglected. The abnormally high temperature hypothesis must be checked with actual knot [O III] $\lambda 4363/\lambda 5007$ measurements or perhaps with the temperature-sensitive [Ar III] $\lambda 5192/\lambda 7136$ ratio before other possible causes for the anomalous [Ar III] emission can be ruled out. In any case, the unusual spectra indicate that the knots are extraordinary in nature compared with most other filamentary material in the Crab Nebula. All of the spectroscopic observations, including more complete data for all of the knots obtained in 1993 December at the Multiple Mirror Telescope, will be reported and discussed at length in a subsequent paper.

We gratefully acknowledge useful discussions with P. A. Hughes and J. Arons.

REFERENCES

- Cault, A., Woodgate, B. E., Brown, L. W., Gull, T. R., Hintzen, P., Lowenthal, J. D., Oliverson, R. J., & Ziegler, M. M. 1992, ApJ, 388, 301
 Davidson, K., & Fesen, R. A. 1985, ARA&A, 23, 119
 Fesen, R. A., Martin, C. L., & Shull, J. M. 1992, ApJ, 399, 599
 Henry, R. B. C., & MacAlpine, G. M. 1982, ApJ, 258, 11
 MacAlpine, G., Lawrence, S., & Brown, B. 1993, BAAS, 25, 785
 MacAlpine, G. M., McGaugh, S. S., Mazzarella, J. M., & Uomoto, A. 1989, ApJ, 342, 364 (MMMU)
 Massey, P., Strobel, K., Barnes, J., & Anderson, E. 1988, ApJ, 328, 315
 Michel, F. C., Scowen, P. A., Dufour, R. J., & Hester, J. J. 1991, ApJ, 368, 463
 Osterbrock, D. E. 1989, in *Astrophysics of Gaseous Nebulae and Active Galactic Nuclei* (Mill Valley: University Science Books), 119
 Scott, J. S., Holman, G. D., Ionson, J. A., & Papadopoulos, K. 1980, ApJ, 239, 769
 Uomoto, A., & MacAlpine, G. M. 1987, AJ, 93, 1511 (UM)
 van den Bergh, S. 1970, ApJ, 160, L27
 Wyckoff, S., & Murray, C. A. 1977, MNRAS, 180, 717 (WM)